www.lajss.org
Latin American Journal of Solids and Structures 6 (2009) 51–72

Solution of the stochastic beam bending problem by Galerkin Method and the Askey-Wiener scheme

Cláudio Roberto Ávila da Silva Júnior[1], André Teófilo Beck[2,*] and Edison da Rosa[3]

[1]DAMEC, Universidade Tecnológica Federal do Paraná. Avenida Sete de Setembro 3165, Curitiba, Paraná, Brasil.
[2]Engenharia de Estruturas, EESC, USP. Av. Trabalhador Sancarlense, 400, São Carlos, SP.
[3]GRANTE/POSMEC, Universidade Federal de Santa Catarina. Trindade, Florianópolis, Santa Catarina, Brasil.

Abstract

In this paper, the Askey-Wiener scheme and the Galerkin method are used to obtain approximate solutions to the stochastic beam bending problem. The study addresses Euler-Bernoulli beams with uncertain bending stiffness modulus. The uncertainty is represented as a parameterized stochastic process. The space of approximate solutions is built using results of density between the space of continuous functions and Sobolev spaces. From the approximate solution, first and second order moments of the response are derived, and compared with the corresponding estimates obtained via Monte Carlo simulation. Results show very fast convergence to the exact solution, at excellent accuracies.

Keywords: Euler-Bernoulli beam, Galerkin method, Askey-Wiener scheme, stochastic processes.

1 Introduction

The field of stochastic mechanics has been subject of extensive research and significant developments in recent years. Stochastic mechanics incorporates the modeling of randomness or uncertainty in the mathematical formulation of mechanics problems. This is in contrast to the more established field of structural reliability, where uncertainty and randomness are also addressed, but where problem solutions are obtained mainly based on deterministic mechanics models.

The analysis of stochastic engineering systems has received new impulse with use of finite element methods to obtain response statistics. Initially, finite element solutions where combined with the Monte Carlo method, and samples of random system response where obtained. Perturbation and Galerkin methods where used in this context [2]. Such methods allowed representation of uncertainty in system parameters or in loads by means of stochastic processes.

*Corresp. author email: atbeck@sc.usp.br Received 16 May 2008; In revised form 24 Nov 2008

At the end of the 80's, Spanos and Ghanem [18] used the Galerkin finite element method to solve a stochastic beam bending problem, where Young's modulus was modeled as a Gaussian stochastic process. The space of approximate solutions was built using the finite element method and chaos polynomials. These polynomials form a complete system in $L^2(\Omega, \mathcal{F}, P) = \overline{\Psi}^{L^2(\Omega,\mathcal{F},P)}$, where $\Psi = span[\{\psi\}_{i=0}^{\infty}]$ is the space generated by the chaos polynomials and $(\Omega, \mathcal{F}, P)$ is a probability space. The ideas presented in this study where innovative and represented a new method to solve stochastic problems.

Babuska et al. [4] presented a stochastic version of the Lax-Milgram lemma. The paper presents a hypothesis which represents limitations to the modeling of uncertainty via Gaussian processes. For certain problems of mechanics, use of Gaussian processes can lead to loss of coercivity of the bi-linear form associated to the stochastic problem. This difficulty was indeed encountered in the study of Silva Jr. [14], and resulted in non-convergence of the solution for the bending of plates with random parameters. This non-convergence was due to the choice of a Gaussian process to represent the uncertainty in some parameters of the system. This failure to converge also affects solutions based on perturbation or simulation methods.

In the paper by Xiu and Karniadakis [8] the Askey-Wiener scheme was presented. This scheme represents a family of polynomials which generate dense probability spaces with limited and unlimited support. This increases the possibilities for uncertain system parameter modeling. In the study, uniform parameterized stochastic processes are considered.

In recent years, much effort is being addressed at representing uncertainty in stochastic engineering systems via non-Gaussian processes. The stochastic beam bending problem has been studied by several authors. Vanmarcke and Grigoriu [19] studied the bending of Timoshenko beams with random shear modulus. Elishakoff et al. [12] employed the theory of mean square calculus to construct a solution to the boundary value problem of beam bending with stochastic bending modulus. Ghanem and Spanos [10] used the Galerkin method and the Karhunem-Loeve series to represent uncertainty in the bending modulus by means of a Gaussian process. Chakraborty and Sarkar [7] used the Neumann series and Monte Carlo simulation to obtain statistical moments of the displacements of curved beams, with uncertainty in the elasticity modulus of the foundation. Although they present numerical solutions for stochastic beam problems, none of the papers referenced above address the matter of existence and uniqueness of the solutions.

In the present paper, the Galerkin method is used to obtain approximate solutions for the bending of Euler-Bernoulli beams with random parameters. The uncertainty of Young modulus is represented by parameterized random processes [11]. The approximated solution space is constructed using isomorphism properties between Sobolev and product spaces, using density between continuous functions and Sobolev spaces and using spaces generated by L^2 polynomials of the Askey-Wiener scheme [6, 8]. The Askey-Wiener scheme is used to represent the uncertainty and to construct the approximate solution space. Another contribution of this paper is a brief theoretical study about the existence and uniqueness of the solution of stochastic

beam bending problem, through the Lax Milgram lemma [4]. The Galerkin solution developed herein is evaluated by comparing first and second order moments of random beam displacement response with the same statistics evaluated via Monte Carlo simulation.

2 Bending of Stochastic Euler-Bernoulli Beams

In this section, the strong and weak formulations of the problem of stochastic bending of Euler-Bernoulli beams are presented. At the end of this section, the Lax-Milgram lemma is used to present a proof of existence and uniqueness of the solution. The strong form of the stochastic beam bending problem is given as:

$$\begin{cases} \frac{d^2}{dx^2}\left(E.I\left(x,w\right)\cdot\frac{d^2u}{dx^2}\right)=f,\forall\left(x,w\right)\in\left(0,L\right)\times\Omega \\ u\left(0\right)=u\left(L\right)=0 \\ \frac{d^2u}{dx^2}\left|_{x=0}=\frac{d^2u}{dx^2}\right|_{x=L}=0 \end{cases} \tag{1}$$

where E is the Young's modulus, I is the moment of inertia, Ω is a sample space and f is a load term. Product $E.I$ is simply referred to as the beam bending stiffness. For the qualitative analysis regarding existence and uniqueness of the response, the following hypotheses are considered:

H1: $\exists c,C\in\mathbb{R}^{+}:P\left(\omega\in\Omega:E.I\left(x,\omega\right)\in\left[c,C\right],\forall x\in\left[0,L\right]\right)=1$

H2: $f\in L^{\infty}\left(\Omega,\mathcal{F},P;L^{2}\left(0,L\right)\right)$

Hypothesis H1 ensures that the beam stiffness modulus is positive-defined and uniformly limited in probability [4]. Hypothesis H3 ensures that the stochastic load process has finite variance.

2.1 Existence and uniqueness of the solution

In this section, a brief theoretical study of existence and uniqueness of the solution of the stochastic Euler-Bernoulli beam bending problem, with uncertainty in the bending stiffness, is presented. For operators with derivatives of order greater than two, no such study was found in the literature. Classical results from functional analysis are used in this study [1, 4, 21]. In order to study existence and uniqueness, the abstract variational problem associated to the strong form (Eq. 1) needs to be defined. The abstract variational problem associated to the beam bending problem defined in Eq. (1) is defined in $V=L^{2}\left(\Omega,\mathcal{F},P;Q\right)$, with $Q=\left\{u\in H^{2}\left(0,L\right)\left|u\left(0\right)=u\left(L\right)=0\wedge\frac{d^2u}{dx^2}\right|_{x=0}=\frac{d^2u}{dx^2}\Big|_{x=L}=0\right\}$,

$$L^{2}\left(\Omega,\mathcal{F},P;Q\right)=\left\{u:\left(0,L\right)\times\Omega\rightarrow\mathbb{R}\left|u\text{ is measurable and }\int_{\Omega}\left\|u\left(\omega\right)\right\|_{H^{2}(0,L)}^{2}dP\left(\omega\right)<+\infty\right.\right\} \tag{2}$$

Expression (2) means that an element $u \in L^2(\Omega, \mathcal{F}, P; Q)$ for $\omega \in \Omega$, fixed, $u(\cdot, \omega) \in Q$. On the other hand, for $x \in (0, L)$, fixed, $u(x, \cdot) \in L^2(\Omega, \mathcal{F}, P)$. Defining the tensorial product between $v \in L^2(\Omega, \mathcal{F}, P)$ and $w \in Q$ as $u = v.w$, one should note that for fixed $\omega \in \Omega$,

$$u(\cdot, \omega) = v(\cdot).w(\omega) \in Q$$

whereas for a fixed $x \in (0, L)$,

$$u(x, \cdot) = v(x).w(\cdot) \in L^2(\Omega, \mathcal{F}, P).$$

Hence, one has

$$L^2(\Omega, \mathcal{F}, P; Q) \simeq L^2(\Omega, \mathcal{F}, P) \otimes Q \Rightarrow V \simeq L^2(\Omega, \mathcal{F}, P; Q) \otimes Q.$$

It is also necessary to redefine the differential operator for the space obtained via tensorial product. The operator $D^{\alpha}_{\omega} : V \to L^2(\Omega, \mathcal{F}, P) \otimes L^2(0, L)$, Matthies and Keese [16], acts over an element $u \in V$ the following way:

$$D^{\alpha}_{\omega} u : \left(\frac{d^{\alpha} v}{dx^{\alpha}}\right)(x).w(\omega), \tag{3}$$

where $\alpha \in \mathbb{N}$ and $\alpha \leq 2$. V is a Hilbert space, with internal product defined as

$$(u, v)_V = \int_{\Omega} \left[\left(D_{\omega} u(\omega), D_{\omega} v(\omega)\right)_{L^2(0,L)} + \left(D^2_{\omega} u(\omega), D^2_{\omega} v(\omega)\right)_{L^2(0,L)} \right] dP(\omega), \tag{4}$$

The internal product defined in Eq. (4) induces the V norm $\|u\|_u = (u, v)^{1/2}_V$, following Kinderlehrer and Stampacchia [15]. The bilinear form $B : V \times V \longrightarrow \mathbb{R}$ is defined as,

$$B(u, v) = \int_{\Omega} \left(E.I.D^2_{\omega} u(\omega), D^2_{\omega} v(\omega)\right)_{L^2(0,L)} dP(\omega) \tag{5}$$

The abstract variational problem associated to the strong form (Eq. 1) is defined as follows:

$$\begin{cases} \text{Find } u \in V \text{ such that} \\ B(u, v) = \langle f, v \rangle, \forall v \in V. \end{cases} \tag{6}$$

From the hypotheses of limited probability one can show that the bilinear form has the following properties:
a. continuity

$$|B(u, v)| \leq C \int_{\Omega} \left\| D^2_{\omega} u(\omega) \right\|_{L^2(0,L)} \left\| D^2_{\omega} v(\omega) \right\|_{L^2(0,L)} dP(\omega) \leq C \|u\|_V \|v\|_V ; \tag{7}$$

b. coercivity

$$\begin{aligned} B(u,u) &\geq c\int_{\Omega}\left(D_{\omega}^{2}u(\omega),D_{\omega}^{2}u(\omega)\right)_{L^{2}(0,l)}dP(\omega) \\ &\geq \frac{c}{2}\int_{\Omega}\left[\left\|D_{\omega}^{2}u(\omega)\right\|_{L^{2}(0,L)}^{2}+\left\|D_{\omega}^{2}u(\omega)\right\|_{L^{2}(0,L)}^{2}\right]dP(\omega) \\ &\geq c\int_{\Omega}\left[\left\|D_{\omega}^{2}u=(\omega)\right\|_{L^{2}(0,L)}^{2}\right]dP(\omega)=c\left\|u\right\|_{V}^{2} \end{aligned} \tag{8}$$

From hypothesis H1 and H2, which state the continuity and coercivity of the bilinear form, and from the Lax-Milgram lemma, it is guaranteed that the problem defined in Eq. (1) has an unique solution, and continuous dependency on the data [4, 5].

3 Uncertainty Representation

In most engineering problems, complete statistical information about uncertainties is not available. Sometimes, the first and second moments are the only information available. The probability distribution function is defined based on experience or heuristically. In this paper, the uncertainty on beam bending stiffness is modeled by uniform random variables.

In order to apply Galerkin's method, an explicit representation of the uncertainty is necessary. In this paper, the Askey-Wiener scheme is used to represent uncertainty and in the construction of the problems solution space.

3.1 The Askey-Wiener scheme

The Askey-Wiener scheme is a generalization of chaos polynomials, also known as Wiener-chaos. Chaos polynomials were proposed by Wiener [20] to study statistical mechanics of gases. Xiu and Karniadakis [8] have shown the close relationship between results presented by Wiener [20] and Askey and Wilson [3] for the representation of stochastic processes by orthogonal polynomials. Xiu and Karniadakis [8] extended the studies of Ghanem and Spanos [10] and Ogura [17] for polynomials belonging to the Askey-Wiener scheme.

The Cameron-Martin theorem [6] shows that Askey-Wiener polynomials form a base for a dense subspace of second order random variables $L^{2}(C,\mathcal{F},P)$. Let $H\subseteq L^{2}(\Omega,\mathcal{F},P)$ be a separable Gaussian Hilbert space and $P_{n}(H)$ be the vector space spanned by all polynomials of order less than n:

$$P_{n}(H)=\left\{\Gamma\left(\{\xi_{i}\}_{i=1}^{N}\right):\Gamma\text{ is the polynomial of order}\leq n;\xi_{i}\in H,\forall i=1,\ldots,N;N<\infty\right\} \tag{9}$$

and

$$H^{:n:} = \overline{P}_n(H) \bigcap \overline{P}_{n-1}(H)^{\perp}, \tag{10}$$

where $\overline{P}_n$ is the closure of P_n . The space $H^{:n:}$ is known as homogeneous chaos of order n. For $n = 0$ one has $H^{:0:} = \overline{P}_0(H)$ the space of constants and $H^{:-1} = \overline{P}_{-1}(H) = \{0\}$. Space $P(H) = \bigcup_{n\in\mathbb{N}} P_n(H)$ is a dense subspace in $L^q(\Omega, \mathcal{F}, P)$ with $q \in \mathbb{N}$. As shown by Jason [13], $L^2(\Omega, \mathcal{F}, P)$ can be decomposed as:

$$L^2 = \oplus_0^{\infty} H^{:n:} \tag{11}$$

Equation (11) is an orthogonal decomposition of $L^2(\Omega, \mathcal{F}, P)$, known as Wiener-chaos decomposition or simply chaos decomposition. One application of this decomposition is the representation of an element $X \in L^2(\Omega, \mathcal{F}, P)$ in terms of elements $X_n \in H^{:n:}$:

$$X = \sum_{n=0}^{\infty} X_n. \tag{12}$$

Equation (12) represents an important result for the approximation theory applied to stochastic systems. Solution of a stochastic system is expressed as a non-linear function in terms Gaussian random variables. This function is expanded in terms of chaos polynomials as:

$$u_i(\omega) = \sum_{p\geq 0} \sum_{n_1+\ldots+n_r=p} \sum_{i_1,\ldots,i_r} u_{i_1\ldots i_r}^{j_1\ldots j_r} \Gamma_p(\xi_{i_1}(\omega), \ldots, \xi_{t_r}(\omega)), \tag{13}$$

where Γ_p is the chaos polynomial of order p and $u_{i_1\ldots i_r}^{j_1\ldots j_r}$ are the polynomial coefficients. The super-index refers to the number of occurrences of $\xi_{i_k}(\omega)$. Chaos polynomials of order p are formed by an Hermite polynomial, in standard Gaussian variables $\{\xi_{i_k}(\omega)\}_{k=1}^r$ of order less than p. Introducing a mapping in the sets of indexes $\{i_k\}_{k=1}^r$ and $\{j_k\}_{k=1}^r$, Eq. (13) can be rewritten as:

$$u_i(\omega) = \sum_{j=1}^{\infty} u_{ij} \psi_j(\xi(\omega)). \tag{14}$$

The internal product between polynomials ψ_i and ψ_j in $L^2(\Omega, \mathcal{F}, P)$ is defined as:

$$(\psi_i, \psi_j)_{L^2(\Omega,\mathcal{F},P)} = \int_{\mathbb{R}^N} (\psi_i.\psi_j)(\xi(\omega)) \, dP(\omega), \tag{15}$$

where dP is a probability measure. These polynomials form a complete ortho-normal system with respect to the probability measure, with the following properties:

$$\psi_0 = 1, (\psi_i, \psi_j)_{L^2(\Omega,\mathcal{F},P)} = \delta_{ij}, \forall i, j \in \mathbb{N}. \tag{16}$$

It is important to observe that in Eq. (15) the polynomials are orthogonal with respect to the standard Gaussian density function of vector ξ . The convergence rate is exponential for the case where the random variable is Gaussian. For other random variables the convergence rate is smaller.

The Askey-Wiener scheme represents a family of sub-spaces generated by orthogonal polynomials obtained from ordinary differential equations [8]. Among them, the Hermite, Laguerre, Jacobi and Legendre polynomials can be cited. Every sub-space generated by these polynomials is a complete system in L^2 . The elements of different sub-spaces of the Askey scheme are inter-related. Figure (1) illustrates the Askey-Wiener scheme through the different polynomial families and the inter-relations between them.

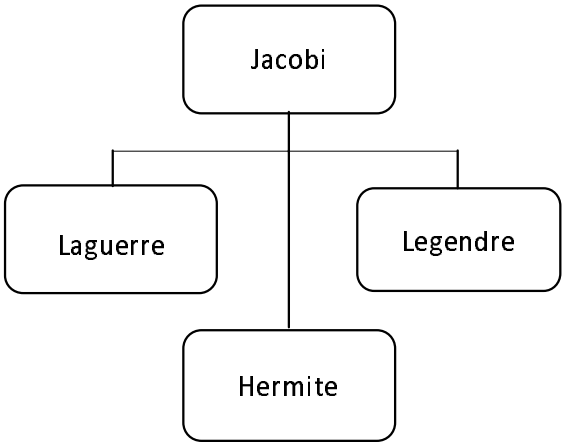

Figure 1: The Askey-Wiener scheme.

The orthogonality between the polynomials is defined with respect to a weight function, which is identical to the probability density function of a certain random variable. For example, the Gaussian density function is used as weight function to obtain the orthogonality between Hermite polynomials. Table (1) shows the correspondence between subsets of polynomials of the Askey-Wiener scheme and the corresponding probability density functions.

The proposal of the Askey-Wiener scheme is to extend the result presented in Eq. (12) to other types of polynomials. The fact that $P_n(H) = span[\{\varphi_i\}_{t=1}^{\infty}]$ with $\varphi_i \in \mathcal{S}$, $\forall i \in \mathbb{N}$ where $\mathcal{S} = \bigcup_{n\in\mathbb{N}} P_n(H)$ is a family of polynomials of the Askey-Wiener scheme and $\mathcal{H}$ is a separable Hilbert space of finite variance random variables.

4 Galerkin Method

The Galerkin method is used in this paper to solve the stochastic beam bending problem with uncertainty in the beam stiffness modulus. It is proposed that approximated solutions to the

Table 1: Correspondence between some random variables and polynomials of the Askey-Wiener scheme.

Random variable	**Polynomial**	**Weight function**	**Support**
Gaussian	Hermite	$e^{-\frac{\|\xi\|^2}{2}}$	$(-\infty,+\infty)$
Gama	Laguerre	$\frac{1}{\Gamma(\alpha+1)}\xi^{\alpha}e^{-\xi}$	$[0,+\infty]$
Beta	Jacobi	$\frac{2^{-(\alpha+\beta+1)}\Gamma(\alpha+\beta+2)}{\Gamma(\alpha+1)\Gamma(\beta+1)}(1-\xi)^{\alpha}(1+\xi)^{\beta}e^{-\xi}$	$[a,b]$
Uniform	Legendre	$\frac{1}{b-a}$	$[a,b]$

stochastic displacement response of the beam have the following form:

$$u(x,\omega)=\sum_{i=1}^{\infty}u_i\delta_i(x,\omega), \tag{17}$$

where $u_i\in\mathbb{R},\forall i\in\mathbb{N}$ are coefficients and $\delta_i\in V$ are the test functions. Numerical solutions to the variational problem defined in Eq. 6 will be obtained. Hence, it becomes necessary to define spaces less abstract than those defined earlier, but without compromising the existence and uniqueness of the solution. From the theory of Sobolev spaces we have $\overline{C^2(0,L)}^{Q}=Q$ and from the theory of chaos polynomials and the Askey-Wiener scheme one has $\overline{\mathcal{S}}^{L^2(\Omega,\mathcal{F},P)}=L^2(\Omega,\mathcal{F},P)$. Consider two complete orthogonal systems $\Phi=span[\{\phi_i\}_{i=1}^{\infty}]$ and $\Psi=span[\{\psi_i\}_{i=1}^{\infty}]$, such that $\overline{\Phi}^{Q}=Q$, $\overline{\Psi}^{s}=\mathcal{S}$, and define the tensorial product between Φ and $\mathcal{S}$ as:

$$(\phi\otimes\psi)_i(x,\omega)=\phi_j(x).\psi_k(\omega),\ \text{with } j,k\in\mathbb{N} \tag{18}$$

To simplify the notation, we will use $\delta_i=(\phi\otimes\psi)_i$. Since approximated numerical solutions are derived in this paper, the solution space has finite dimensions. This implies truncation of the complete orthogonal systems Φ and $\mathcal{S}$. Hence one has $\Phi_m=span[\{\phi_i\}_{i=1}^{m}]$ and $\Psi_n=span[\{\psi_i\}_{i=1}^{n}]$, which results in $V_M=\Phi_m\otimes\Psi_n$. With the above definitions and results, it is proposed that numerical solutions are obtained from truncation of the series expressed in Eq. 13 at the M^{th} term:

$$u_M(x,\omega)=\sum_{i=1}^{M}u_i\delta_i(x,\omega). \tag{19}$$

Substituting Eq. (17) in Eq. (4), one arrives at the approximated variational problem:

$$\begin{cases} \text{Find } \{u_i\}_{i=1}^{M} \in \mathbb{R}^M \text{ such that} \\ \sum_{i=1}^{M}\sum_{k=1}^{N} \mathcal{B}_k\left(\delta_i,\delta_j\right) u_i = \langle f,\delta_j\rangle\,,\ \forall \delta_j \in V_M \end{cases} \tag{20}$$

where

$$\mathcal{B}_k\left(\delta_i,\delta_j\right) = \int_{\Omega}\int_{0}^{L} \varphi_k\xi_k D_{\omega}^2\delta_j . D_{\omega}^2\delta_j dx dP\left(\omega\right) \text{ and } \langle f,\delta j\langle = \int_{\Omega}\int_{0}^{L} f.\delta_j dx dP\left(\omega\right) \tag{21}$$

The approximated variational problem (Eq. 20) consists in establishing the coefficients of the linear combination expressed in Eq. (19). Using a vector-matrix representation, the system of linear algebraic equations defined in Eq. (20) can be written as:

$$\mathbf{KU} = \mathbf{F} \tag{22}$$

where $\mathbf{K} \in \mathbf{M}_M(\mathbb{R})$ is the stiffness matrix, $\mathbf{U} = \{u_i\}_{i=1}^{M}$ is the displacement vector and $\mathbf{F} = \{f_i\}_{i=1}^{M}$ is the loading vector. The sparseness of the stiffness matrixes for example 1 (to be presented) is shown in Figure (2). Remember that "p" is the degree of the chaos polynomial.

The stiffness matrix corresponding to Figure 2(a) has dimension 20 and nz = 188 (number of nonzero elements), whereas the matrix corresponding to Figure 2(b) has dimensions 56 and nz = 1142. The conditioning number (n_C) corresponding to these two matrixes is $n_C = 610.9443$ and $n_C = 936.3786$, respectively. These numbers show that the conditioning number increases with the dimension of the approximation space. This can lead to ill-conditioning of the of the stiffness matrix and hence to the loss of accuracy of the approximated solution. In this paper, a family of Legendre polynomials is used to construct space Ψ_n , defined in the variables $(\xi_1,\xi_2) \in [-1,1]\times[-1,1]$.

5 Statistical Moments

Numerical solutions to be obtained are defined in $V_M \subset L^2\left(\Omega,\mathcal{F},P\right)\otimes Q$. Interest lies in the statistical moments of the stochastic displacement response. In this section, it is shown how the first and second order moments are evaluated from the numerical solution.

The statistical moment of k^{th} order of a random variable $u\left(x,\cdot\right)$ is obtained, for a fixed point $x \in [0,L]$, by taking the k^{th} power of the displacement and integrating with respect to it's probability measure:

$$\mu_{u(x)}^{k} = \int_{\Omega} u_M^k\left(x,\omega\right) dP\left(\omega\right) = \overbrace{\sum_{i_1}\ldots\sum_{i_k}}^{k \text{ times}} u_{i_1}\ldots u_{i_k} \int_{\Omega} \left(\delta_{i_1}\ldots\delta_{i_k}\right)\left(x,\xi\left(\omega\right)\right) dP\left(\xi\left(\omega\right)\right) \tag{23}$$

The integration term $dP\left(\cdot\right)$ is a probability measure defined as:

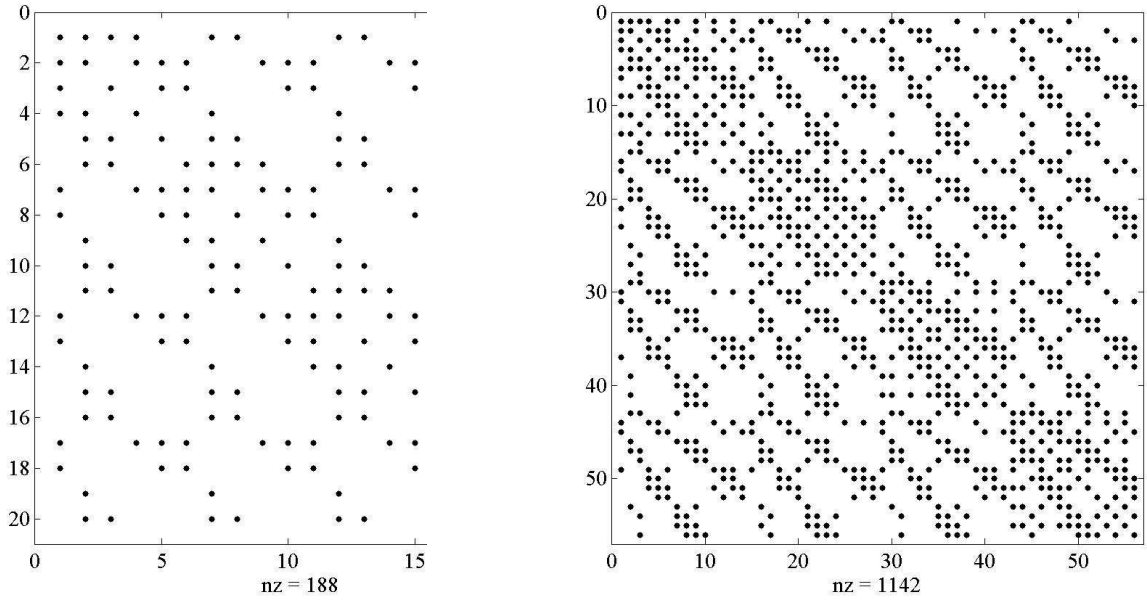

(a) for $m = 4$, $n = 7$, $p = 2$; (b) for $m = 4$, $n = 14$, $p = 4$.

Figure 2: Sparseness of the stiffness matrix of example 1.

$$dP\left(\xi\left(\omega\right)\right) = \prod_{i=1}^{N} \rho_i\left(\xi i\left(\omega\right)\right) d\xi_i\left(\omega\right) \tag{24}$$

where $\rho_i : \xi_i \to \mathbb{R}$ is the probability density function of random variable ξ_i . From the measure and integration theory [9], one knows that the probability measure defined in Eq. (24) is the product measure obtained from the product between probability measure spaces associated to the random variables $\xi\left(\omega\right) = \left\{\xi_i\left(\omega\right)\right\}_{i=1}^{N}$, with $\xi_i : \Omega \to [a_i, b_i]$. With the probability measure defined in Eq. (23) one has:

$$\mu_{u(x)}^{k} = \overbrace{\sum_{i_i} ... \sum_{ik}}^{k \text{ times}} u_{i_1} ... u_{i_k} \int_{a_1}^{b_1} ... \int_{a_N}^{b_N} \left(\delta_{i_1} ... \delta_{i_k}\right)\left(x, \xi\left(\omega\right)\right) \rho_1\left(\xi_1\right) ... \rho_N\left(\xi_N\right) d\xi_1\left(\omega\right) ... d\xi_N\left(\omega\right) \tag{25}$$

The integrals in Eq. (25) are called iterated integrals. The first order statistical moment, or expected value, of the stochastic displacement process evaluated at a point $x \in [0, L]$ is:

$$\mu_{u(x)} = \sum_{i=1}^{m} u_{(i-1).n+1} \phi_i\left(x\right) \tag{26}$$

The second-order statistical moment (the variance) of this displacement is:

$$V_{u(x)} = \sum_{i=1}^{M}\sum_{j=1}^{M} u_i u_j \int_{a_1}^{b_1} ... \int_{a_N}^{b_N} (\delta_i.\delta_j)(x,\xi(\omega))\,\rho_1(\xi_1)...\rho_N(\xi_N)\,d\xi_1(\omega)...d\xi_N(\omega) - \sum_{i=1}^{m}\sum_{j=1}^{m} u_{(i-1).n+1} u_{(j-1).n+1}(\phi_i.\phi_j)(x) \quad (27)$$

In the numerical example to follow, the statistical moments defined in Eqs. (26 and 27) are evaluated and compared with the same moments obtained via Monte Carlo simulation, using five thousand samples ($N_S = 5000$).

6 Numerical Example

In this section, two numerical examples of the stochastic Euler-Bernoulli beam bending problem are presented. In the first example, uncertainty on the Young modulus is considered. In the second example, the high of the beam's cross-section is assumed uncertain. In both cases, uncertainty is modeled by parameterized stochastic processes. In both examples, the beam is simply supported at both ends, the span (L) equals one meter, the cross-section is rectangular ($b \times h$) with $b = \frac{1}{200}$ m and the beam is subject to an uniform distributed load of $f(x) = 1$KPa.m, $\forall x \in [0,1]$.

The first and second order statistical moments of the numerical solution obtained via Galerkin method are compared with the same moments evaluated via Monte Carlo simulation. To evaluate the error of the approximated solution, the relative error functions in expected value and in variance (ε_{μ_u} and $\varepsilon_{\sigma_u^2}$, respectively), are defined as,

$$\epsilon_{\mu_u}(x) = \begin{cases} (100\%) \times \left|\left(1 - \frac{\mu_u}{\hat{\mu}_u}\right)(x)\right|, & \forall x \in (0,1) \\ 0, & \forall x \in \{0,1\} \end{cases} \wedge \epsilon_{\sigma_u^2}(x) = \begin{cases} (100\%) \times \left|\left(1 - \frac{\sigma_u^2}{\hat{\sigma}_u^2}\right)(x)\right|, & \forall x \in (0,1) \\ 0, & \forall x \in \{0,1\} \end{cases} \quad (28)$$

where μ_u and σ_u^2 , are the Galerkin-based expected value and variance, respectively, and $\hat{\mu}_u$ and $\hat{\sigma}_u^2$ are the Monte Carlo estimates of the same moments. Numerical results presented in this paper were obtained in a HP Pavilion personal computer, running a MATLAB computational code.

6.1 Example 1: random Young's modulus

In this example, the Young's modulus of the material is modeled as a parameterized stochastic process:

$$E(x,\omega) = \mu_E + \sqrt{3}.\sigma_E\left[\xi_1(\omega)\,cos(x) + \xi_2(\omega)\,sen(x)\right], \quad (29)$$

where μ_E is the mean value, σ_E is the standard deviation and $\{\xi_1, \xi_2\}$ are independent uniform random variables. The mean value $\mu_E = 210GPa$ is adopted in the solution. Numerical solutions are obtained for two values of the standard deviation: (a) $\sigma_E = \left(\frac{1}{10}\right).\mu_E$; (b) $\sigma_E = \left(\frac{1}{5}\right).\mu_E$. The beams cross-section has width $b = \frac{1}{200}$m and hight $h = \frac{1}{100}$m . The covariance function of Young's modulus for case (a) is presented in Fig. 3.

It can be observed in the figure that stochastic process Young's modulus is strictly stationary. The covariance function shown in Fig. 3 is obtained in exact form from Eq. 29 and from the orthogonality property of random variables $\{\xi_1, \xi_2\}$.

Figure 4(a) shows all the sampled realizations of the random transversal displacement of the beam. Figure 4(b) shows the displacements at mid-spam for $x = \frac{1}{2}$.

Figure 5 shows the expected value of the displacement for the beam 5(a) and the relative error in expected value 5(b). The expected value is evaluated via Galerkin method for $p \in \{1, 2, 3, 4\}$. The error in expected value is computed by comparing these results with results of Monte Carlo simulation. In Figure 5(a) it can be seen that for $p \geq 2$ the Galerkin results accumulates over the Monte Carlo simulation solution. Figure 5(b) shows the relative error of approximated Galerkin solutions. Results accumulate over each other for $p \geq 3$.

Fig. 6 shows the covariance function of the displacement. The figure shows that the displacement stochastic process is not strictly stationary. This means that the problems linearity did not preserve, for the displacement process, the stationarity of the Young's modulus.

In Figure 7 the variance of random beam displacement is shown. Figure 7(a) shows the variance obtained via approximated Galerkin solution for $p \in \{1, 2, 3, 4\}$. Figure 7(b) shows the relative error of Galerkin solutions, in comparison to simulation results.

The convergence behaviors for expected value and variance are quite similar, but it is observed that relative errors for variance are slightly larger than the errors in expected value. This is expected since the approximations for the response moments loose quality as the order of the moment increases.

The convergence rate of the numerical solutions is very good. Relative error functions in expected value and in variance decrease considerably when the degree of polynomial interpolation goes from $p = 1$ to $p = 2$. A smaller reduction is observed when the polynomial order is increased from $p = 3$ to $p = 4$.

Summary of results for cases (a) and (b):

Results of expected value, variance and corresponding relative errors for the random variable obtained by fixing $x = \frac{1}{2}$ in the random process displacement, for cases (a) and (b) of example 1, are summarized in Table 2. Results are presented for approximated solutions with $p \in \{1, 2, 3, 4\}$. Monte Carlo estimates of expected value and variance for cases (a) and (b) where obtained as:

- $\hat{\mu}_{u\left(\frac{1}{2}\right)} = -0.014980290850853$ m;

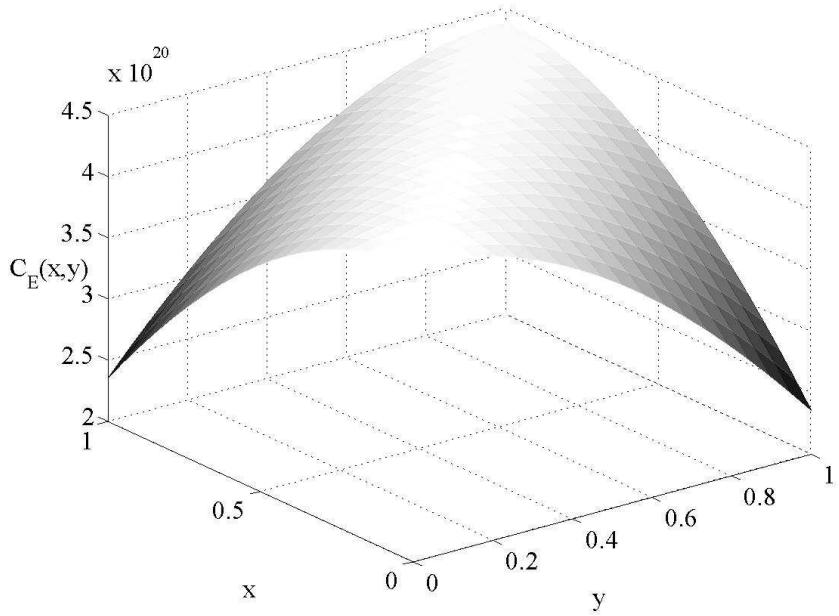

Figure 3: Covariance function of Young's modulus for case (a).

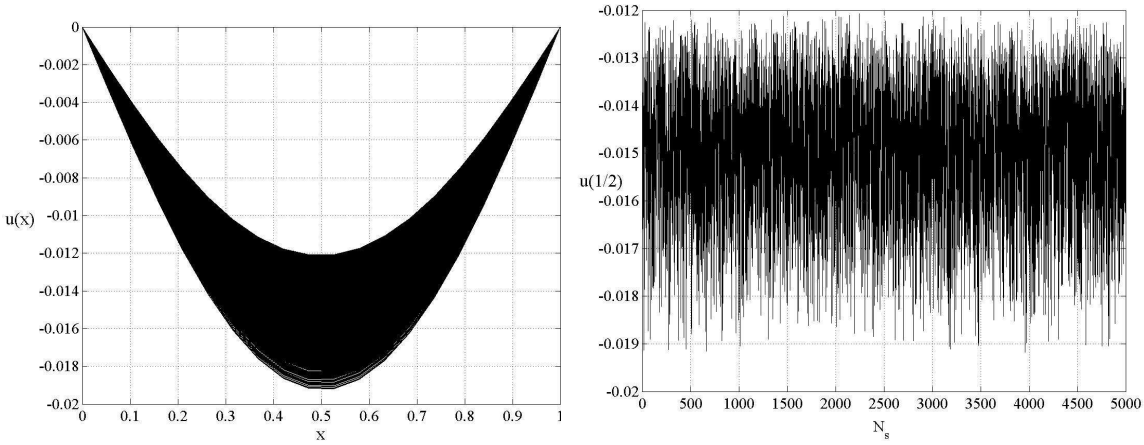

(a) (b)

Figure 4: a) Realizations of the displacement random process; b) Realizations of random variable $u\left(\frac{1}{2}\right)$

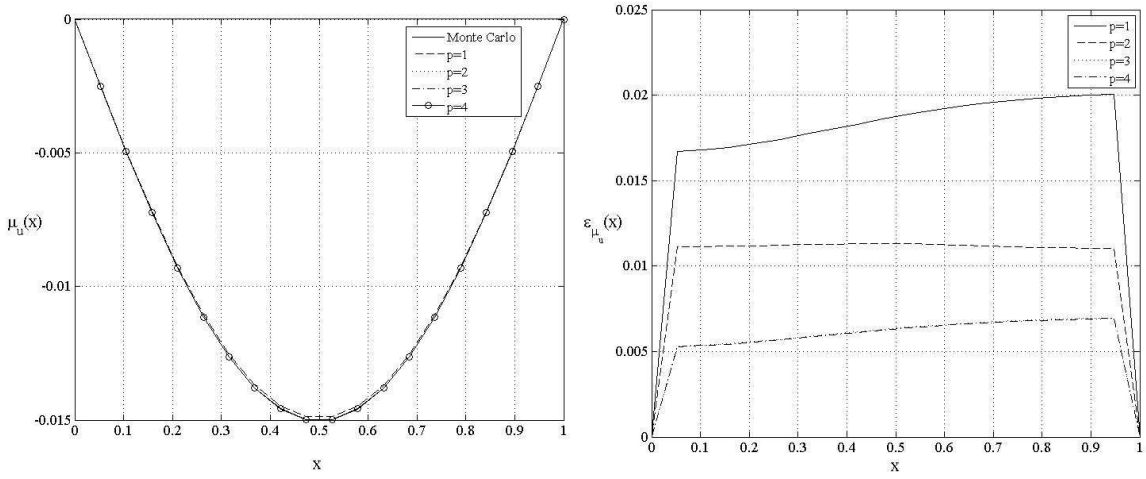

(a) (b)

Figure 5: a) Expected value of the displacement; b) Relative error in expected value.

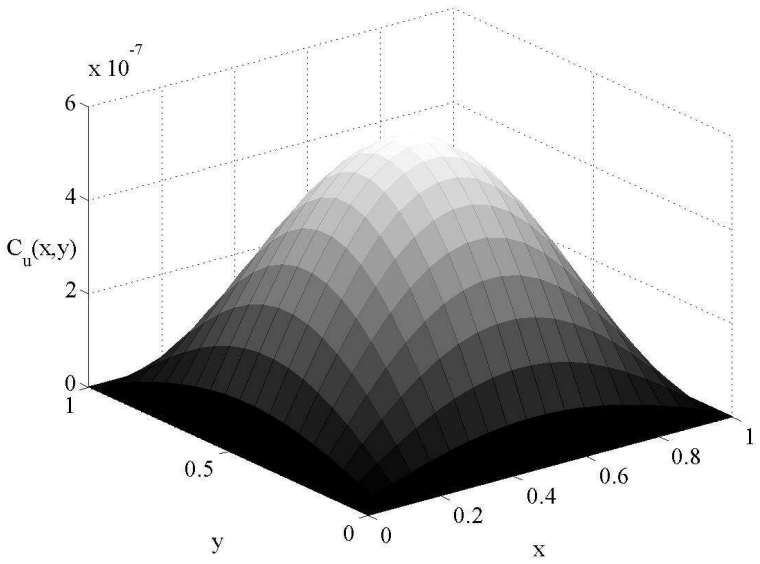

Figure 6: Covariance function of the displacement.

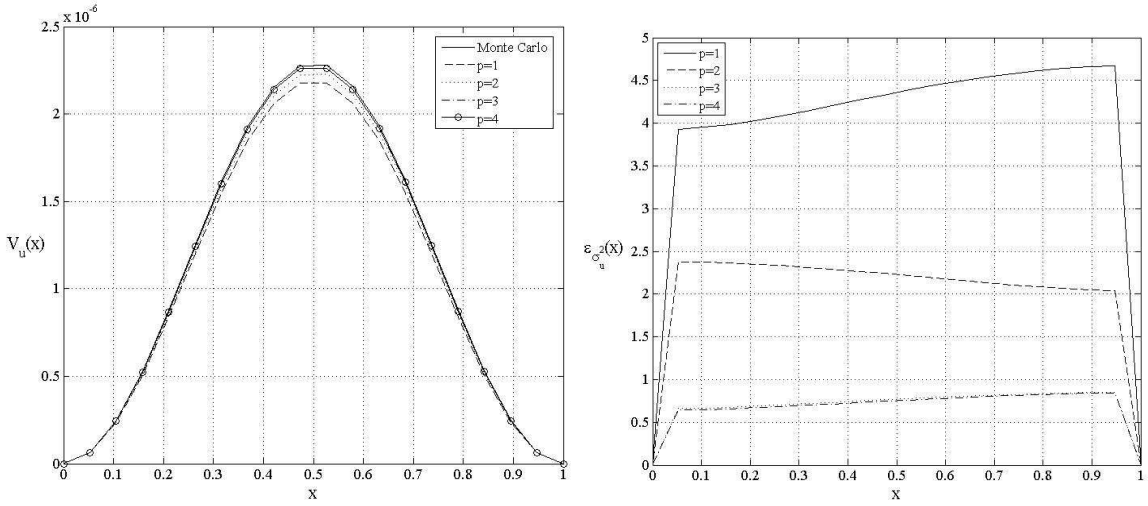

(a) (b)

Figure 7: a) Variance of the displacements; b) Relative error in variance.

$\hat{\sigma}^2_{u(\frac{1}{2})} = 2.27603016058937 \times 10^{-6}$ m^2;

and

- $\hat{\mu}_{u(\frac{1}{2})} = -0.0154842703449571$ m;
- $\hat{\sigma}^2_{u(\frac{1}{2})} = 1.09773390470067 \times 10^{-5}$ m^2.

It is observed in Table 2 that an increase in the Young's modulus variance resulted in an increase in the variance of transversal beam displacement. The expected value of the displacement was expected to be the same in the two cases studied. In other words, the expected value of the displacement was not expected to change by changing variance of Young's modulus. This should be the consequence of representing Young's modulus as a deterministic term added to a random term with zero mean. Hence, the (expected) correspondence between the deterministic part of Young's modulus and the mean displacement was not observed. This is observed in the approximated (Galerkin) and in the Monte Carlo solutions. In all cases, the relative error in variance is larger than the relative error in expected values. In terms of expected value, case (a) presented the smallest relative error.

6.2 Example 2: random cross-section height

In this second example, the height of beams cross-section is represented as a parameterized stochastic process:

Table 2: Summary of numerical results for cases (a) and (b) of example 1: expected value, variance, relative errors in expected value and variance for the random displacement response at mid-spam $\left(x = \frac{1}{2}\right)$.

p	**case(a)**			
	$\mu_{u_M\left(\frac{1}{2}\right)}$	$\sigma^2_{u_M\left(\frac{1}{2}\right)}$	$\varepsilon_{\mu_u}\left(\frac{1}{2}\right)$	$\varepsilon_{\sigma^2_u}\left(\frac{1}{2}\right)$
1	-0.014977505506094	$2.1774709978363 \times 10^{-6}$	0.018593395727389	4.33031004859571
2	-0.0149785968021307	$2.22500740117425 \times 10^{-6}$	0.0113085168981607	2.24174355413215
3	-0.0149793492220302	$2.2586733753253 \times 10^{-6}$	0.00628578464963902	0.762590301508722
4	-0.0149793541761291	$2.25903752370874 \times 10^{-6}$	0.00625271387097294	0.746591023917982
p	**case (b)**			
	$\mu_{u_M\left(\frac{1}{2}\right)}$	$\sigma^2_{u_M\left(\frac{1}{2}\right)}$	$\varepsilon_{\mu_u}\left(\frac{1}{2}\right)$	$\varepsilon_{\sigma^2_u}\left(\frac{1}{2}\right)$
1	-0.0154455459627453	$9.26275145950668 \times 10^{-6}$	0.250088517890467	15.6193370739294
2	-0.0154648167456578	$1.01397468943761 \times 10^{-5}$	0.125634588301266	7.63019297339668
3	-0.0154793536198963	$1.08605558745147 \times 10^{-5}$	0.0317530303417188	1.06385684173525
4	-0.0154798078358090	$1.08984821070522 \times 10^{-5}$	0.0288196282338699	0.718361158536607

$$h\left(x,w\right) = \mu_h + \sqrt{3}.\sigma_h\left[\xi_1\left(\omega\right)cos\left(x\right) + \xi_2\left(\omega\right)sen\left(x\right)\right], \tag{30}$$

where μ_h is the mean value, σ_h is the standard deviation and $\{\xi_1, \xi_2\}$ are independent uniform random variables. The mean value $\mu_h = \frac{1}{100}$m is adopted in the solution. Numerical solutions are obtained for two values of the standard deviation: (a) $\sigma_h = \left(\frac{1}{10}\right).\mu_h$; (b) $\sigma_h = \left(\frac{1}{5}\right).\mu_h$. The covariance function for random process beam height is similar to the previous example.

Figure 8(a) shows all the sampled realizations of the random transversal displacement of the beam. Figure 8(b) shows the displacements at mid-spam for $x = \frac{1}{2}$.

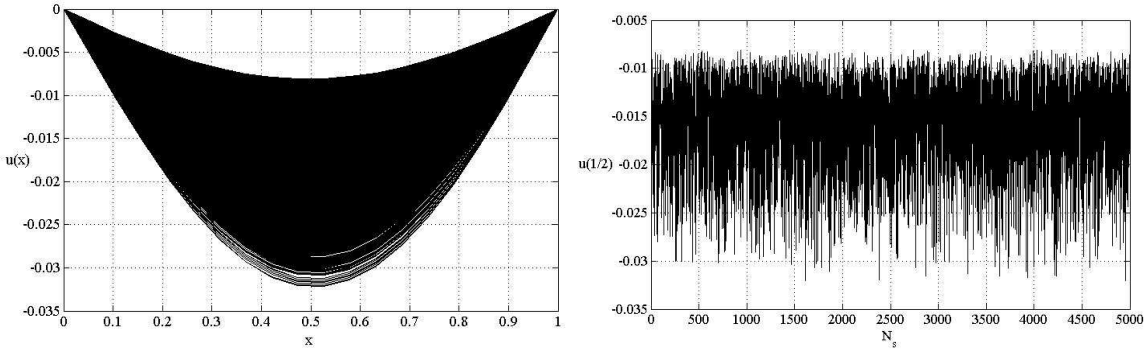

(a) (b)

Figure 8: a) Realizations of the displacement random process; b) Realizations of random variable $u\left(\frac{1}{2}\right)$

A comparison of results in Figures 4 and 8 shows larger dispersion of transversal displacements for random beam height. Hence, uncertainty propagation was larger for random beam height in comparison to random beam stiffness.

Figure 9(a) shows the expected value of displacements for the beam. Two results are shown in the figure: Monte Carlo simulation and the numerical (Galerkin) results. In Fig. 9(a) it is observed that results obtained via Galerkin solutions for $p \geq 2$ accumulate over the Monte Carlo estimate. Fig. 9(b) shows that indeed the relative error in expected value is largely reduced for $p \geq 2$. A comparison of Figures 5(b) and 9(b) shows that the relative error in expected values is greater for the random height problem than for the case of random stiffness coefficient.

Fig. 10 shows the covariance function of transversal beam displacements. As for the previous example, it is observed that the displacement response is not stationary as the beam height random process.

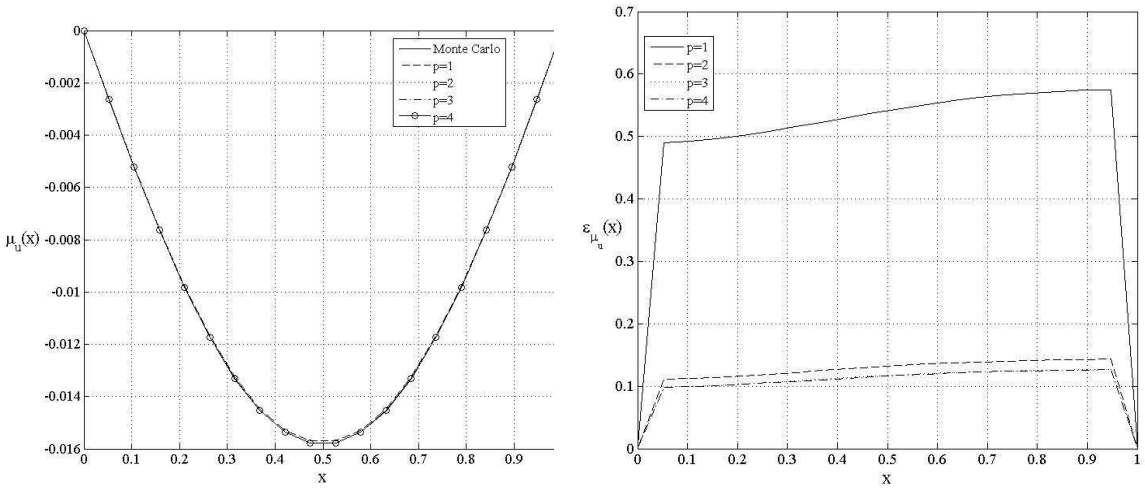

(a) (b)

Figure 9: a) Expected value of the displacement; b) Relative error in expected value.

Figure 11 shows the variance of beam displacements and the relative error in variance, for four degrees of polynomial interpolation. Relative error in variance is significantly larger than relative error in expected value. This is expected since the approximations for the response moments loose quality as the order of the moment increases. Results in figure 11(b) show very fast convergence of the Galerkin solutions. The relative error in both expected value and variance decreases by about 300% when the polynomial degree changes from $p = 1$ to $p = 2$. A smaller reduction is obtained when the degree is changed from $p = 2$ to $p = 3$. The relative error in variance is larger for this example in comparison to the case of random beam stiffness.

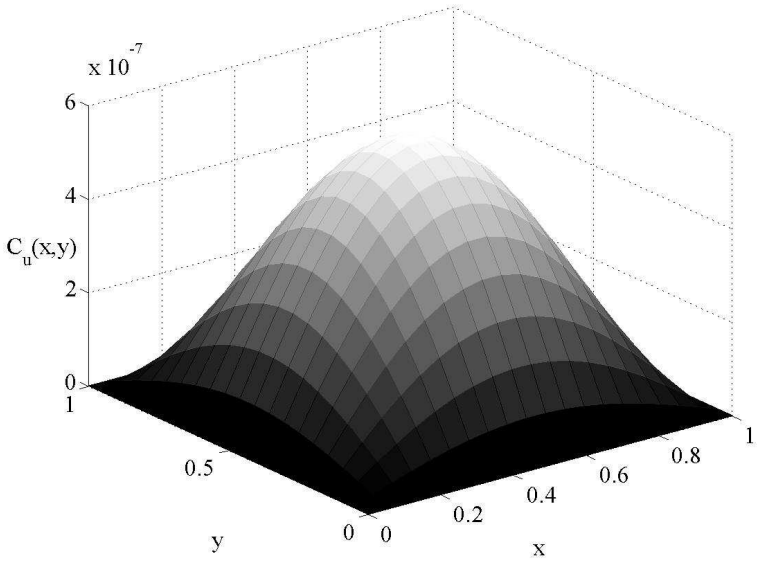

Figure 10: Covariance function of transversal beam displacements.

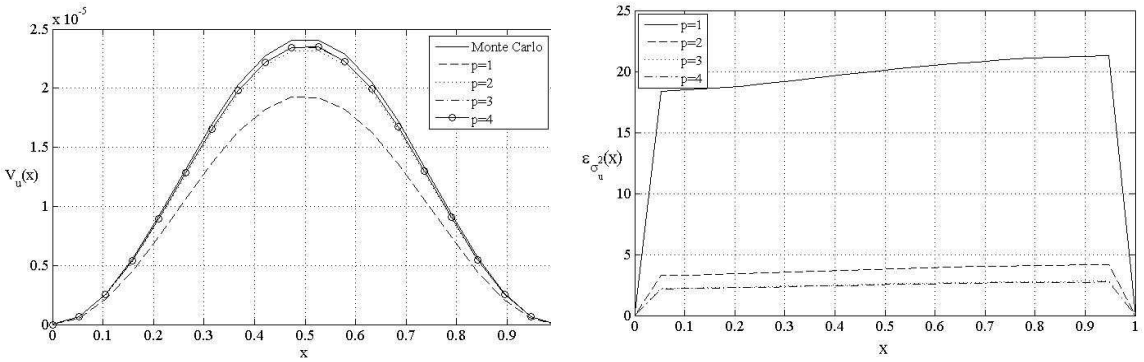

(a) (b)

Figure 11: a) Variance of the displacements; b) Relative error in variance.

Summary of results for cases (a) and (b):

Table 3 summarizes results of expected value, variance and corresponding relative errors for the random variable obtained by fixing $x = \frac{1}{2}$ in the random process displacement, for cases (a) and (b) of example 2. Results are presented for approximated solutions with $p \in \{1, 2, 3, 4\}$. Monte Carlo estimates of expected value and variance for cases (a) and (b) where obtained, respectively, as:

- $\hat{\mu}_{u\left(\frac{1}{2}\right)} = -0.0157871470471983$ m;

$\hat{\sigma}^2_{u\left(\frac{1}{2}\right)} = 2.40357009946749 \times 10^{-5}$ m^2 ;
and

- $\hat{\mu}_{u\left(\frac{1}{2}\right)} = -0.0195763835699485$ m;
- $\hat{\sigma}^2_{u\left(\frac{1}{2}\right)} = 19.8054679939951 \times 10^{-5}$ m^2.

Comparing the expected value and variance obtained by approximated solutions with simulation results, one notes that both are smaller than the corresponding Monte Carlo estimates. Table 3 also shows that, for case (a), the expected value and variance of random variable $u\left(\frac{1}{2}, \cdot\right)$ is smaller than for case (b). The same behavior is observed for the Monte Carlo estimates of expected value and variance for this random variable.

For cases (a) and (b) in this example, the relative error in variance was larger than the relative error in expected values. In terms of expected value and variance, case (a) presented the smallest relative error. The expected value of the displacement was expected to be the same in both cases studied. In other words, the expected value of the displacement was not expected to change with varying variance of beam height. This should be the consequence of representing beam height as a deterministic term added to a random term with zero mean. Hence, the (expected) correspondence between the deterministic part of beam height and the mean displacement was not observed. This is observed in the approximated (Galerkin) and in the Monte Carlo solutions. A final point to be noticed is that, in the comparison between cases (a) and (b), the increase in displacement variance resulted larger than the increase in the variance of Young's modulus.

Summary of CPU processing time for both examples

Table 4 shows CPU processing time required in the Galerkin and Monte Carlo solutions of this problem.

In general, it is observed that CPU processing time is smaller for example 1 than for example 2, for Monte Carlo and Galerkin solutions. This result exemplifies increase of computational costs in terms of problem non-linearity. Processing time results show that the Galerkin approximation

Table 3: Summary of numerical results for cases (a) and (b) of example 2: expected value, variance, relative errors in expected value and variance for the random displacement response at mid-spam $\left(x = \frac{1}{2}\right)$

p	**case (a)**			
	$\mu_{u_m\left(\frac{1}{2}\right)}$	$\sigma^2_{u_M\left(\frac{1}{2}\right)}$	$\varepsilon_{\mu_u}\left(\frac{1}{2}\right)$	$\varepsilon_{\sigma^2_u}\left(\frac{1}{2}\right)$
1	-0.0157021984852101	$1.92334463809149\times10^{-5}$	0.538086848334137	19.9796736314196
2	-0.0157665159932702	$2.31288549995655\times10^{-5}$	0.130682598105811	3.77291261573896
3	-0.0157688339676447	$2.34208188684934\times10^{-5}$	0.115999930189177	2.55820342546997
4	-0.0157689030893046	$2.34354117559092\times10^{-5}$	0.115562095159572	2.49749004157871
p	**case (b)**			
	$\mu_{u_m\left(\frac{1}{2}\right)}$	$\sigma^2_{u_M\left(\frac{1}{2}\right)}$	$\varepsilon_{\mu_u}\left(\frac{1}{2}\right)$	$\varepsilon_{\sigma^2_u}\left(\frac{1}{2}\right)$
1	-0.0181301418033707	$7.62653395370197\times10^{-5}$	7.38768609334911	61.492785951767
2	-0.0191855975545909	$15.0243574516819\times10^{-5}$	1.99621147573695	24.1403563084844
3	-0.0193566156021009	$17.7217928733184\times10^{-5}$	1.12261780661566	10.5207063085228
4	-0.0193795679216213	$18.3519099119952\times10^{-5}$	1.00537286482951	7.33917563796342

is advantageous over Monte Carlo simulation for all degrees of polynomial interpolation, for problem 1.

Comparing the quality of results presented in figures 9 and 11 with CPU processing times, it is observed that the Galerkin solution is only justified for interpolation order of up to p=3. This result shows some drawbacks of the Galerkin solution and the Askey-Wiener scheme when applied to problems involving strong non-linearity in the uncertain parameters.

7 Conclusions

In this paper, theoretical and practical results for bending of stochastic Euler-Bernoulli beams have been presented. The Lax-Milgram lemma was used for a theoretical study about the existence and uniqueness of the solution. A Galerkin solution of stochastic Euler-Bernoulli beam bending problems was developed. The approximated solution space was constructed by the tensorial product between measure spaces of finite dimensions. The family of Legendre polynomials, derived from the Askey-Wiener scheme, was used to construct the solution space.

The proposed methodology was used to solve two numerical problems, one considering an uncertain Young's modulus and one assuming an uncertain cross-section height. In both examples, the uncertainty was represented by parameterized stochastic processes, using polynomials of the Askey-Wiener scheme. From the approximated Galerkin solutions, statistical moments

Table 4: CPU processing time for Galerkin and Monte Carlo, solutions of examples 1 and 2, cases (a) and (b).

Example (case)	**CPU time [s], Monte Carlo simulation**	**CPU time [s], Galerkin method**			
		$p = 1$	$p = 2$	$p = 3$	$p = 4$
1 (a)	180.969	10.39	10.47	37.12	96.01
1 (b)	180.203	10.26	10.56	34.78	94.72
2 (a)	842.531	142.81	200.34	697.83	2452.20
2 (b)	858.797	138.74	187.06	672.03	2416.47

of first and second order of transversal beam displacements were evaluated. The performance of Galerkin approximations was evaluated by comparing these moments with the corresponding statistics obtained via Monte Carlo simulation.

For the problem considering an uncertain bending stiffness, the Askey-Wiener Galerkin solution presented very good convergence rates, and excellent accuracy. The approximated Galerkin solution with polynomial order $p = 2$ resulted in very accurate results, for a fraction of the CPU computation time required for the Monte Carlo simulation.

For the problem where uncertainty was considered on cross section height, convergence of approximated Galerkin solutions was slower, and accuracy was not as good. This results from the strong nonlinearity of the problem, which intensifies propagation of the uncertainty to the random beam response. The Askey-Wiener Galerkin solution developed herein was not as efficient for this problem, as it was for the linear problem (with uncertain bending stiffness). However, an accurate solution was still obtained, at smaller processing times when compared to Monte Carlo, for polynomial interpolation of order $p = 3$. In general, it was observed that the approximation looses quality as the order of the computed moment increases.

The Askey-Wiener Galerkin solution developed herein is a theoretically sound and efficient method for the solution of stochastic problems in engineering. Use of the Askey-Wiener scheme in representing parameter uncertainty and in the construction of approximated solution spaces was shown to be an efficient strategy for the solution of stochastic beam bending problems.

References

[1] R. A. Adams. *Sobolev spaces*. Academic Press, New York, 1975.

[2] J.M. Araújo and A.M. Awruch. On stochastic finite elements for structural analysis. *Computers and Structures*, 52(3):461–469, 1994.

[3] R. Askey and J. Wilson. *Some Basic Hypergeometric Polynomials that Generalize Jacobi Polynomials*. AMS, Mem. Amer. Math. Soc. 319 Providence, RI., 1985.

[4] I. Babuska, R. Tempone, and G. E. Zouraris. Solving elliptic boundary value problems with uncertain coefficients by the finite element method: the stochastic formulation. *Computer Methods in Applied Mechanics and Engineering*, 194(12-16):1251–1294, 2005.

[5] S. C. Brenner and L. R. Scott. *The Mathematical Theory of Finite Element Methods*. Springer-Verlag, 1994.

[6] R. H. Cameron and W. T. Martin. The orthogonal development of nonlinear functionals in series of Fourier-Hermite functionals. *Annals Mathematics*, 48:385–392, 1947.

[7] S. Chakraborty and Sarkar S. K. Analysis of a curved beam on uncertain elastic foundation. *Finite Elements in Analysis and Design*, 36(1):73–82, 2000.

[8] Xiu D. and Karniadakis G.E. The Wiener-Askey Polynomial Chaos for Stochastic Differential Equations. *SIAM J. Sci. Comput.*, 24(2):619–644, 2002.

[9] P. J. Fernandez. *Measure and Integration (in Portuguese)*, page 198. IMPA, 2002.

[10] R. Ghanem and P.D. Spanos. *Stochastic Finite Elements: A Spectral Approach*. Dover, NY, 1991.

[11] M. Grigoriu. *Applied Non-Gaussian Processes: Examples, Theory, Simulation, Linear Random Vibration, and Matlab Solutions*. Prentice Hall, 1995.

[12] Elishakoff I., Ren Y. J., and Shinozuka M. Some exact solutions for the bending of beams with spatially stochastic stiffness. *International Journal of Solids and Structures*, 32(16):2315–2327, 1995.

[13] S. Jason. *Gaussian Hilbert Spaces*. Cambridge University Press, 1997.

[14] Silva Jr. and C. R. A. *Application of the Galerkin method to stochastic bending of Kirchhoff plates (in Portuguese)*. Florianpolis, SC, Brazil, 2004. Doctoral Thesis, Department of Mechanical Engineering Federal University of Santa Catarina.

[15] D. Kinderlehrer and G. Stampacchia. *An Introduction to Variational Inequalities and Their Applications*, page 313. Society for Industrial Mathematics, 1987.

[16] H. G. Matthies and Keese A. Galerkin methods for linear and nonlinear elliptic stochastic partial differential equations. *Computer Methods in Applied Mechanics and Engineering*, 194(12-16):1295–1331, 2005.

[17] H. Ogura. Orthogonal functionals of the Poisson process. *IEEE Trans. Inform. Theory*, 18(4):473–481, 1972.

[18] P. D. Spanos and R. Ghanem. Stochastic finite element expansion for media random. *Journal Engineering Mechanics*, 125(1):26–40, 1989.

[19] E. H. Vanmarcke and M. Grigoriu. Stochastic finite element analysis of simple beams. *Journal of Engineering Mechanics*, 109(5):1203–1214, 1983.

[20] N. Wiener. The homogeneous chaos. *American Journal Mathematics*, 60:897–936, 1938.

[21] K. Yoshida. *Functional analysis*. Springer, Berlin, 1978.